ARTICLE

Chemical Dynamics Simulations of the Hydroxyl Radical Reaction with Ethene[†]

Jiaxu Zhang[a*], Li Yang[b], Diego Troya[c]

a. Beijing National Laboratory for Molecular Sciences, Institute of Chemistry, Chinese Academy of Sciences, Beijing 100190, China
b. Technical Institute of Physics and Chemistry, Chinese Academy of Sciences, Beijing 100190, China
c. Department of Chemistry, Virginia Tech, Blacksburg, VA 24061, USA

(Dated: Received on October 23, 2013; Accepted on December 10, 2013)

We present a theoretical study of the reaction of the hydroxyl radical with ethene using electronic structure calculations and direct-dynamics simulations. High-accuracy electronic structure calculations at the CCSD(T)/aug-cc-pVTZ//MP2/aug-cc-pVDZ level have been carried out to characterize the representative regions of the potential energy surface of various reaction pathways, including OH-addition and H-abstraction. These *ab initio* calculations have been employed to derive an improved set of parameters for the MSINDO semiempirical Hamiltonian specific to the $OH+C_2H_4$ reaction. The specific-reaction-parameter Hamiltonian captures the *ab initio* data accurately, and has been used to perform direct quasiclassical trajectory simulations of the $OH+C_2H_4$ reaction at collision energies in the range of 2−10 kcal/mol. The calculated cross sections reveal that the OH-addition reaction dominates at all energies over H-abstraction. In addition, the excitation function of addition is reminiscent of a barrierless capture process, while that for abstraction corresponds to an activated one, and these trends can be connected to the transition-state energies of both reactions. We note that the development of an accurate semiempirical Hamiltonian for the $OH+C_2H_4$ reaction in this work required the inclusion of empirical dispersion corrections, which will be important in future applications for which long-range intermolecular attraction becomes significant.

Key words: QCT, SRP Hamiltonian, MSINDO, Hydroxyl, Ethene

I. INTRODUCTION

The hydroxyl radical is important in combustion processes and atmospheric chemistry. OH is the most important daytime atmospheric oxidant and plays an important role in cleansing the troposphere via reactions with volatile organic compounds (VOCs), which are emitted into the atmosphere either from combustion processes or non-anthropogenically [1−3]. To a large extent, the amount of alkenes in the atmosphere is governed by their reactions with hydroxyl radical, and in turn, the reactions with alkenes play a role in controlling the concentration of hydroxyl radical in atmosphere.

Interpreting experiments on the dynamics and kinetics of reactions of OH with alkenes by either statistical calculations or chemical dynamics simulations requires accurate potential energy surfaces (PESs) [4−8]. Despite extensive theoretical and computational investigations of the ground-state reaction pathways and rate constants for the $OH+C_2H_4$ reaction [9−17], none of these studies investigated the reaction dynamics in regions away from the minimum-energy reaction path of the PES. Nevertheless, it has been shown that the $OH+C_2H_4$ reaction is dominated by electrophilic addition of the OH radical to the π bond that yields a CH_2CH_2OH collision complex, with hydrogen abstraction becoming significant at higher temperatures [9, 10, 16, 17]. The OH-addition mechanism leads to a complicated dependence of the overall reaction rate constant on pressure and temperature. The hydroxy-adduct formed by OH-addition can be either collisionally stabilized or dissociates back to reagents. Alternatively, the adduct can also undergo possible isomerization and dissociation to yield a variety of products, but only after overcoming significant barriers, which results in slow processes at ambient temperatures. The thermal rate coefficients over a broad range of temperature and pressure have been determined by experiments [1, 9, 10, 18] and theoretical calculations [9−13], with a focus on room-temperature conditions and above.

The characterization of stationary points on a PES typically provides limited insight into chemical reaction

[†]Part of the special issue for "the Chinese Chemical Society's 13th National Chemical Dynamics Symposium".

*Author to whom correspondence should be addressed. E-mail: zhjx2029970@yahoo.com

dynamics since the actual atomic-level dynamics may deviate substantially from that predicted by the stationary points and the minimum-energy path [19, 20]. Illustrative examples of this phenomenon can be provided by the direct and round-about mechanisms for the Cl^-+CH_3I S_N2 reaction [19], and the major non-minimum-energy reaction path that F^-+CH_3OOH reactive collisions follow [21]. The incomplete reaction picture gleaned by the stationary points provides motivation for performing chemical dynamics simulations of OH+alkenes reactions. In turn, dynamics calculations will serve to augment the limited information provided by earlier kinetic studies. In this work, we perform a direct-dynamics study of the $OH+C_2H_4$ reaction using a specific-reaction-parameters (SRP) semiempirical Hamiltonian derived from *ab initio* data. To our knowledge, this is the first time that a full-dimensional dynamics study is carried out for this reaction.

Direct-dynamics simulations have been proven very useful for interpreting the kinetics and dynamics of various important chemical reactions [5, 6, 19−31]. In direct dynamics the calculation of the potential energy $V(q)$ and its first derivatives with respect to the atomic coordinates $\partial V/\partial q_i$ required for propagating trajectories are obtained directly from electronic structure calculations without the need for fitting an analytic potential energy function. The major problem with direct dynamics is that a large number ($>10^6$) of energy gradient calculations is needed to obtain statistically significant dynamics results. The need for such a large number of energy gradients restricts common direct-dynamics studies to inexpensive electronic-structure methods with small basis sets. Because the computational overhead of semiempirical Hamiltonians is substantially smaller than most first-principles methods, there is considerable interest in their application in direct-dynamics calculations [32]. While standard semiempirical Hamiltonians generally can not accurately capture the PES due to the neglect and parameterization of expensive electronic integrals and the use of minimal basis sets, these problems can be ameliorated by developing sets of parameters for a specific reaction. SRP Hamiltonians better reproduce high-level quantum-mechanical calculations of the PES [31], and preserve their computational efficiency, which enables extensive and potentially accurate reaction dynamics calculations. Various chemical dynamics simulations have been recently carried out using this SRP technology [24, 25, 27−31, 33].

In this work, by high-level *ab initio* calculations of the PES of $OH+C_2H_4$ reaction and direct dynamics simulations of $OH+C_2H_4$ collisions using SRP Hamiltonian developed from *ab inito* information of PES, we investigated the reaction of OH radical with ethene theoretically.

II. *ab initio* CALCULATIONS

The essential stationary points of the PES for the $OH+C_2H_4$ reaction have been characterized using electronic structure theory. Geometry optimization of reagents, products, minima, and transition states has been performed mainly using second-order MØller-Plesset (MP2) [34, 35] perturbation theory with the correlation-consistent double-zeta basis set of Dunning augmented with diffuse functions (MP2/aug-cc-pVDZ) [36, 37]. The stationary nature of the optimum structures has been corroborated by harmonic vibrational frequency calculations. To confirm that the optimized transition states connect the pertinent minima, intrinsic reaction coordinate (IRC) [38] calculations have also been carried out at the MP2/aug-cc-pVDZ level of theory. In order to obtain more reliable energetic data, single-point energy calculations have been performed at the CCSD(T) [39] level of theory (coupled-cluster approach with single, double and perturbative triple excitations) with the aug-cc-pVTZ [36, 37] basis set using directly the MP2/aug-cc-pVDZ optimized geometries. All calculations have used an unrestricted reference, and have been carried out using the Gaussian 09 package of programs [40].

The schematic of PES of the $OH+C_2H_4$ reaction is depicted in Fig.1. The direct hydrogen abstraction between OH and C_2H_4 through transition state TSRP1 yields products water and vinyl radical (P1). On a different pathway, the initial association of reagents can form a hydrogen-bonded complex C_2H_4-OH (C1), which progresses to the CH_2CH_2OH adduct (im1) after surmounting a small barrier (TSC11). The im1 species can undergo a C−H bond rupture leading to products $HOCHCH_2+H$ (P2). Alternatively, im1 can isomerize either to CH_3CH_2O (im2) via a 1,3-hydrogen shift, or to CH_3CHOH (im3) by a 1,2-hydrogen shift. The im2 species evolves through C−C and C−H bond dissociations to H_2CO+CH_3 (P3) and $OCHCH_3+H$ (P4), respectively, or undergoes a 1,2-hydrogen shift to convert to isomer 3, followed by its dissociation to form P4 (O−H bond breaking) or P2 (C−H bond breaking). As shown in Fig.1, while addition of OH to the double bond to form the im1 species requires a small barrier (TSC11), subsequent reactions from im1 all involve relatively high barriers. This suggests that once the im1 complex is formed, the system might get trapped for a significant period of time in the relatively deep potential well, or even dissociate back to reagents instead of advancing toward products.

Comparison of the barrier of addition to the much higher transition state TSRP1 of the H-abstraction pathway (7.6 kcal/mol) suggests that at low energies abstraction will be not competitive to addition. Several theoretical studies have focused on these two important channels for the $OH+C_2H_4$ reaction. The structures and energies of the key stationary points in these two pathways are given in Fig.2 and Tables I and II, previ-

DOI:10.1063/1674-0068/26/06/765-773

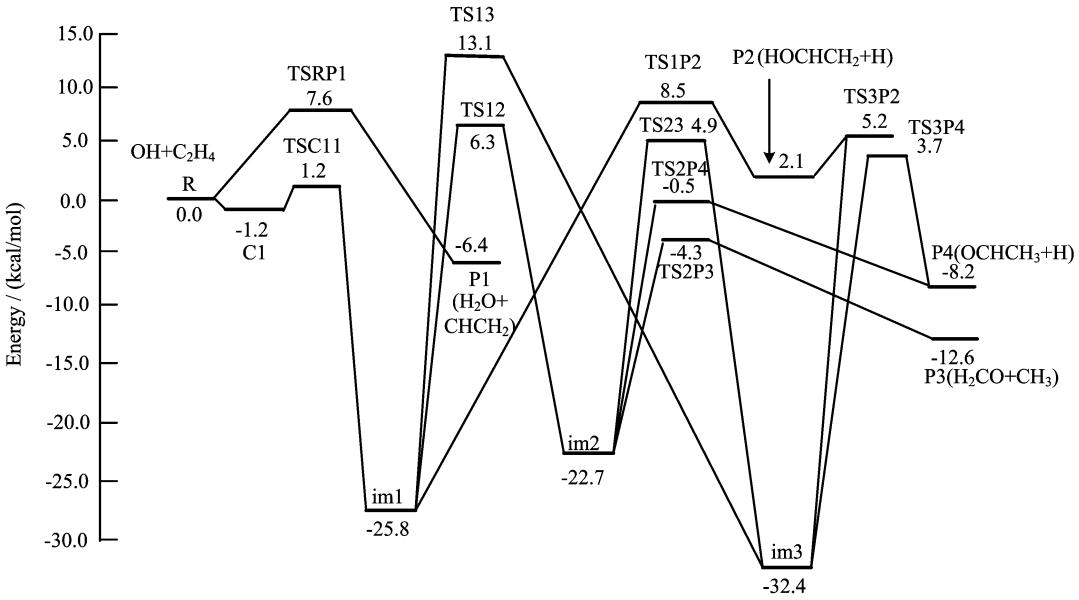

FIG. 1 Potential energy schematic for the OH+C_2H_4 reaction at the CCSD(T)/aug-cc-pVTZ//MP2/aug-cc-pVDZ level of theory. The energy is relative to reagents and includes zero point energy (ZPE) corrections, with the ZPEs calculated at the MP2/aug-cc-pVDZ level. The ZPE for C1 is obtained at the MP2/6-31G(d) level.

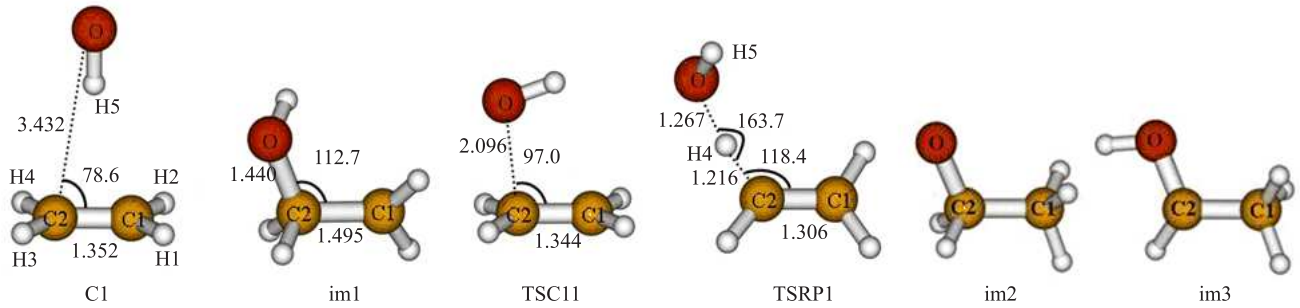

FIG. 2 Geometries of selected stationary points, for the OH-addition and H-abstraction pathways for the OH+C_2H_4 reaction, optimized with the MP2/aug-cc-pVDZ level of theory. Distances are in Å and angles in (°).

TABLE I Calculated energies of selected stationary points for the OH-addition and H-abstraction pathways on the OH+C_2H_4 PES. Energies in kcal/mol are with respect to reagents and include ZPE.

	C1	im1	TSC11	TSRP1
MP2[a]	−1.8[d]	−29.2	6.7	12.0
CCSD(T)//MP2[b]	−1.5[d]	−25.8	1.2	7.6
SRP-MSINDO		−25.1		6.6
RQCIT//QCI[c]	−1.9	−26.2	0.2	4.9

[a] MP2/aug-cc-pVDZ.
[b] CCSD(T)/aug-cc-pVTZ//MP2/aug-cc-pVDZ.
[c] QCISD(T)/cc-pV∞Z//QCISD/6-311++G(d,p) [10].
[d] ZPE calculated at the MP2/6-31G(d) level of theory.

ous results are also given for comparison. The energies of all minima and saddle points obtained at various levels of theory are listed in the supplementary material.

Overall, the geometries of structures optimized with the MP2/aug-cc-pVDZ level are in agreement with prior theoretical results at different levels of theory [9−12, 15]. The largest difference between our MP2 geometries and the QCI results by Senosiain *et al.* [10] is for the C2−O bond length of hydrogen-bonded complex C1, for which our MP2 value is 0.154 Å shorter than that of QCI theory. However, our MP2 C2−O bond length agrees well with the B3LYP/6-311++G(d,p) value reported by Klippenstein *et al.* with the largest difference being 0.050 Å [9]. Senosiain *et al.* also reported the stationary point energies for the OH+C_2H_4 reaction at the RQCIT//QCI level of theory [10]. Our CCSD(T)//MP2 energies agree within 2 kcal/mol with the RQCIT//QCI values in most cases. The largest difference lies in the H-abstraction barrier TSRP1, for which our CCSD(T)//MP2 energy is 2.7 kcal/mol higher than RQCIT/QCI value. We note that the wavefunction of hydrogen-bonded complex C1 shows an instability at the MP2 level with the aug-cc-pVDZ basis

DOI:10.1063/1674-0068/26/06/765-773

TABLE II Representative geometrical parameters of selected stationary points for the OH-addition and H-abstraction pathways of the OH+C_2H_4 reaction[a].

	im1			TSRP1				
	R_{O-C2}/Å	R_{C-C}/Å	∠OC2C1/(°)	R_{O-H4}/Å	R_{C2-H4}/Å	R_{C-C}/Å	∠OH4C2/(°)	∠H4C2C1/(°)
MP2/aug-cc-pVDZ	1.440	1.495	112.7	1.267	1.216	1.306	163.7	118.4
SRP-MSINDO	1.500	1.468	112.0	1.237	1.181	1.340	161.3	120.0

set, which leads to an incorrect ZPE. Thus, the ZPE correction for C1 is calculated using a smaller 6-31G(d) basis set. The subsequent high-level CCSD(T)/aug-cc-pVTZ single-point energy calculation based on the MP2/6-31G(d) geometry of C1 gives the ZPE corrected energy of −1.2 kcal/mol. With this MP2/6-31G(d) ZPE included, the CCSD(T)/aug-cc-pVTZ//MP2/aug-cc-pVDZ energy for C1 is −1.5 kcal/mol, which is in good agreement with RQCIT//QCI value of −1.9 kcal/mol.

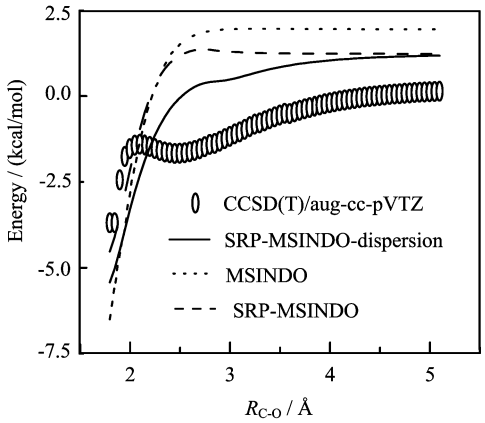

FIG. 3 Potential energy surface profiles of the entrance channel of the OH+C_2H_4→im1 (CH_2CH_2OH) OH-addition reaction calculated at various levels of theory. The graph shows dual-level calculations in which the geometries correspond to MP2/aug-cc-pVDZ calculations.

III. SPECIFIC REACTION PARAMETERS MSINDO HAMILTONIAN

As a low-cost semiempirical method, MSINDO [41, 42] (modified symmetrically orthogonalized intermediate neglect of differential overlap) has been widely used in direct dynamics studies [24, 25, 28−31]. In this section, we show how *ab initio* information for the global PES is used to develop an SRP MSINDO Hamiltonian that is suitable for the OH+C_2H_4 reaction.

An improved parameter set for MSINDO has been derived by using several sets of *ab initio* information on the OH+C_2H_4 PES. First, all of the stationary points of the reaction, including reagents, products, intermediates, and transition states are included in the parameter optimization, with energies at the CCSD(T)/aug-cc-pVTZ level. Secondly, to cover broader swaths of the PES of the OH+C_2H_4 reaction, the key pathway of OH-addition to ethene was considered. To map this region of the PES, we scanned the C2−O coordinate (see Fig.2) from the transition state TSC11 value of 2.096 Å at the MP2/aug-cc-pVDZ level toward reagents at 0.05 Å steps until the C2−O coordinate reached 5.096 Å. In each of the points of the scan, the rest of coordinates were frozen at the MP2/aug-cc-pVDZ transition state values. A similar scan was carried out for the C2−O bond that is formed from its value at TSC11 toward im1 at 0.05 Å steps until the C2−O coordinate reached 1.396 Å. Both scans were performed at the CCSD(T)/aug-cc-pVTZ level. Accurately capturing the approaches in the vicinity of the entrance channel of OH-addition is important for the subsequent dynamics studies, as this region of the PES controls critical dynamics properties of the system, such as the addition/abstraction branching ratio.

In addition to mapping the PES using the scans just described, quasiclassical trajectories starting from reagents OH and C_2H_4 are propagated by using the standard AM1 semiempirical Hamiltonian. In those trajectories, the only pathways identified are either inelastic scattering, or addition to form the im1 CH_2CH_2OH adduct. 592 points are selected from the propagation to appropriately cover the global PES region of OH-addition to ethene. The energies of the points obtained in that trajectory propagation are subsequently recalculated at the CCSD(T)/aug-cc-pVTZ level to obtain a more accurate description of the PES.

Overall, the grid of CCSD(T)/aug-cc-pVTZ calculations just described provides ∼700 *ab initio* points and is employed as a reference in the reoptimization of the parameters of the MSINDO Hamiltonian. The MSINDO parameter optimization was performed using a nonlinear least-squares procedure that minimizes the difference between the CCSD(T)/aug-cc-pVTZ and MSINDO energies. During the parameter optimization, we noted that the classical (non-ZPE corrected) energies of the addition reaction pathway (Fig.3) exhibited long-range attraction before entering into a shallow well prior to the submerged barrier that leads to the im1 species. This long-ranged attraction is primarily due to dispersion interactions, which are typically not described well by semiempirical Hamiltonians, including MSINDO. While we tried to capture the long-ranged attraction via parameter optimization, the low level of theory in the Hamiltonian precludes a proper description of dispersion. However, this long-range attraction

DOI:10.1063/1674-0068/26/06/765-773

TABLE III Original and SRP-MSINDO parameters involved in the OH+C_2H_4 reaction[a] .

Parameter	Original	SRP[b]	Parameter	Original	SRP[b]	Parameter	Original	SRP[b]
ζ_s^U(H)	1.0060	1.2842	K_s(C)	0.0867	0.0933	ζ_s(O)	2.3538	2.6450
ζ_s(H)	1.1576	1.2161	τ_{1s}(C)	5.0830	4.7554	ζ_p(O)	2.1559	2.3322
K_s(H)	0.1449	0.1729	ε_{1s}(C)	10.4300	9.7276	K_s(O)	0.1242	0.0933
I_s(H)	−0.5000	−0.5521	I_s(C)	−0.8195	−0.7321	τ_{1s}(O)	7.3271	6.7051
$\alpha(1)$(H)	0.3856	0.3534	I_p(C)	−0.3824	−0.4056	ε_{1s}(O)	19.5500	27.2596
$\alpha(2)$(H)	0.5038	0.4765	$\alpha(1)$(C)	0.4936	0.4637	I_s(O)	−1.6838	−2.1959
ζ_s^U(C)	1.6266	1.4278	$\alpha(2)$(C)	0.6776	0.8095	I_p(O)	−0.5780	−0.64351
ζ_p^U(C)	1.5572	1.5898	ζ_s^U(O)	2.1109	2.0416	$\alpha(1)$(O)	0.2485	0.2812
ζ_s(C)	1.7874	1.3952	ζ_p^U(O)	1.9055	1.7899	$\alpha(2)$(O)	0.2246	0.1815
ζ_p(C)	1.6770	1.7562						

[a] For a definition of parameters, please see Ref.[41].
[b] Dispersion corrections are involved in the SRP development.

potentially plays an important role in the reaction dynamics, as it might steer reagents toward the im1 products at low collision energies [43]. Therefore, neglecting a good description of this region of the PES might result in incorrect dynamics behavior.

To help solve the lack of dispersion in MSINDO, an empirical damped dispersion correction was added in the spirit of similar approaches to DFT methods. The chosen dispersion correction [44, 45] using van der Waals radii, atomic dispersion coefficients and its functional form is given by

$$E_{\rm disp} = -\sum_{i,j<i}^{N_{\rm atoms}} f_{\rm damp}(R_{ij})\frac{C_{ij}}{R_{ij}^6} \quad (1)$$

where $N_{\rm atoms}$ is the total number of atoms, R_{ij} is the interatomic distance between atoms i and j, and the C_{ij} is the geometric mean of the atomic dispersion coefficients C_i and C_j:

$$C_{ij} = (C_i C_j)^{1/2} \quad (2)$$

The function $f_{\rm damp}$ damps the dispersion correction for shorter interatomic distances and has the form:

$$f_{\rm damp}(R_{ij}) = \frac{1}{1+\exp\left[-\alpha\left(\dfrac{R_{ij}}{R_{\rm vdW}^i + R_{\rm vdW}^j} - 1\right)\right]} \quad (3)$$

where $R_{\rm vdW}^i$ and $R_{\rm vdW}^j$ are the van der Waals radii for atoms i and j, and α is a parameter that is usually set to 23 [44]. The atomic $R_{\rm vdW}$ are 1.001, 1.452, and 1.342 Å for atoms H, C, and O, and the atomic dispersion coefficients C are 0.14, 1.75, and 0.70 nm^{6}J/mol, respectively [45].

Inclusion of this dispersion correction in the MSINDO Hamiltonian allows for a better fit of the *ab initio* data, as shown in Fig.3. The SRP-MSINDO parameters obtained after the optimization procedure are compared to the original parameters in Table III. The relative differences between both sets of parameters are very small, and in no case the new SRP-MSINDO parameters differ from the original ones by more than a factor of 2. The resulting SRP-MSINDO energies agree reasonably well with the CCSD(T)/aug-cc-pVTZ values for the grid of ∼700 *ab initio* points included in the fitting process with a mean square root deviation of ∼2 kcal/mol. Figure 3 shows a more quantitative comparison between the original MSINDO, SRP-MSINDO with or without dispersion correction, and the *ab initio* CCSD(T)/aug-cc-pVTZ energies in the PES region of OH-addition entrance channel. Compared with the original MSINDO, the SRP-MSINDO Hamiltonian better describes the potential energy curve, and with the dispersion correction included, the SRP-MSINDO Hamiltonian reproduces reasonably well the high-quality CCSD(T)/aug-cc-pVTZ energies. A more detailed look at the CCSD(T)/aug-cc-pVTZ data shows that the energy drops smoothly from the reagents' asymptote towards a very shallow minimum. This minimum precedes the transition state, whose energy is below reagents. In contrast, both the original and SRP-MSINDO PES connect reagents and the addition minimum through a continuously downhill pathway. Notwithstanding, the reactions are classically barrierless with both methods, and the absolute energy differences between SRP-MSINDO and CCSD(T)/aug-cc-pVTZ are rather small, especially compared to the total energies involved in the reaction dynamics study that we present below.

As shown in Table II, the structures of stationary points obtained at the SRP-MSINDO level are in good agreement with the MP2/aug-cc-pVDZ results, with the bond length and angle deviation being not more than 0.06 Å and 3°, respectively. The calculated SRP-MSINDO frequencies of reactants are listed in Table IV and generally agree well with the experimental values with the average deviation of ∼7%. The stationary-

DOI:10.1063/1674-0068/26/06/765-773

TABLE IV SRP-MSINDO frequencies (in cm^{-1}) of reactant C_2H_4 and in comparison with experimental values[a].

Mode	SRP	Exp. [51]	Mode	SRP	Exp. [51]	Mode	SRP	Exp. [51]
b2u CH_2 rock	929	826	b3g CH_2 rock	1163	1236	b1u CH_2 str	3332	2989
b2g CH_2 wag	973	943	ag CH_2 scis	1406	1342	ag CH_2 str	3379	3026
b3u CH_2 wag	1024	949	b1u CH_2 scis	1453	1444	b3g CH_2 str	3445	3103
au CH_2 twist	1131	1023	ag CC str	1939	1623	b2u CH_2 str	3451	3106

[a] SRP-MSINDO and Exp. [50] frequencies for sg OH str are 3492 and 3738 cm^{-1}, respectively.

point energy differences between SRP-MSINDO and CCSD(T)/aug-cc-pVTZ are less than 1 kcal/mol. As can be seen from Table I, remarkably, SRP-MSINDO provides energies that are closer to CCSD(T)/aug-cc-pVTZ than the much more computationally expensive MP2/aug-cc-pVDZ results.

The SRP Hamiltonian derived in this way, including the dispersion correction, was used to perform trajectory calculations of the $OH+C_2H_4$ reaction, which we present in the following section.

IV. DIRECT DYNAMICS SIMULATIONS

Direct-dynamics trajectory calculations, with the SRP-MSINDO Hamiltonian derived above, have been performed to investigate the dynamics of the hydroxyl radical reaction with the ethene molecule. The initial separation between reagents is set to 15.0 a.u. to ensure that the initial interaction energies are negligible. The trajectories are terminated typically after a maximum of 5×10^3 integration steps with an integration time step of 0.24 fs, or when the separation between the reaction products exceeds 16 a.u.

To investigate the dependence of reaction dynamics on the initial collision energies $E_{\rm coll}$, the simulations have been performed at $E_{\rm coll}$ of 2, 4, 6, 8, and 10 kcal/mol. The value of the maximum sampling impact parameter $b_{\rm max}$ for each $E_{\rm coll}$ has been found by incrementing b gradually until no reaction occurs out of 2×10^3 trajectories. The resulting values of $b_{\rm max}$ chosen in this manner are shown in Fig.4 and Fig.S1 (supplementary material). Initial coordinates and momenta for the reagents have been generated via normal-mode sampling from the VENUS program [46, 47]. Batches of 10^4 trajectories have been calculated at each collision energy.

A. Opacity functions

The opacity functions, *i.e.*, the probability $P(b)$ of OH-addition and H-abstraction reaction pathways at impact parameter b, versus impact parameter, have been calculated at different collision energies. The representative opacity functions at 2 and 10 kcal/mol are plotted in Fig.4, and the results at 4−8 kcal/mol are shown in Fig.S1 (supplementary material). Under all conditions, the reaction probabilities for OH-addition are significantly larger than those for abstraction. The differences are especially large at the lowest collision energy, where the probability of abstraction is negligible. There are also remarkable differences in the opacity functions for OH addition according to whether dispersion corrections are included at low collision energy. The dispersion correction makes possible the reaction of slowly approaching reagents at impact parameters much longer (b>5 a.u.) than the case when no dispersion corrections are included. The intuitive picture emerging from this result is one in which reagents attract each other at long range toward the transition state when dispersion is included. This behavior is reminiscent of capture-type dynamics, and it is not so obviously present when the dispersion is neglected.

At larger collision energies, study of the opacity functions shows that the dispersion correction plays a far less significant role than that at 2 kcal/mol collision energy. In effect, at $E_{\rm coll}$=10 kcal/mol the reaction probabilities with or without dispersion become more comparable, both in their values at the same impact parameters, and in the range of impact parameters that lead to reaction. This is not unexpected, since at higher $E_{\rm coll}$ the much larger relative velocity between the reagents will overwhelm the weak attractive interactions between reagents.

B. Reaction cross sections

Figure 5 exhibits the calculated cross sections of OH-addition and H-abstraction pathways as a function of collision energies. Clearly, OH-addition dominates over H-abstraction at all collision energies. The cross section dependence on collision energy is slightly different for abstraction and addition. For abstraction, the excitation function shows a threshold and the cross sections grow with collision energy, which is consistent with an activated process. On the other hand, there seems to be no threshold for addition, and the cross sections at low collision energy seem to go through a slight minimum and increase as collision energy decreases. This behavior is expected in a barrierless reaction with capture-type dynamics.

As shown in Fig.5, the effects of dispersion on the

DOI:10.1063/1674-0068/26/06/765-773

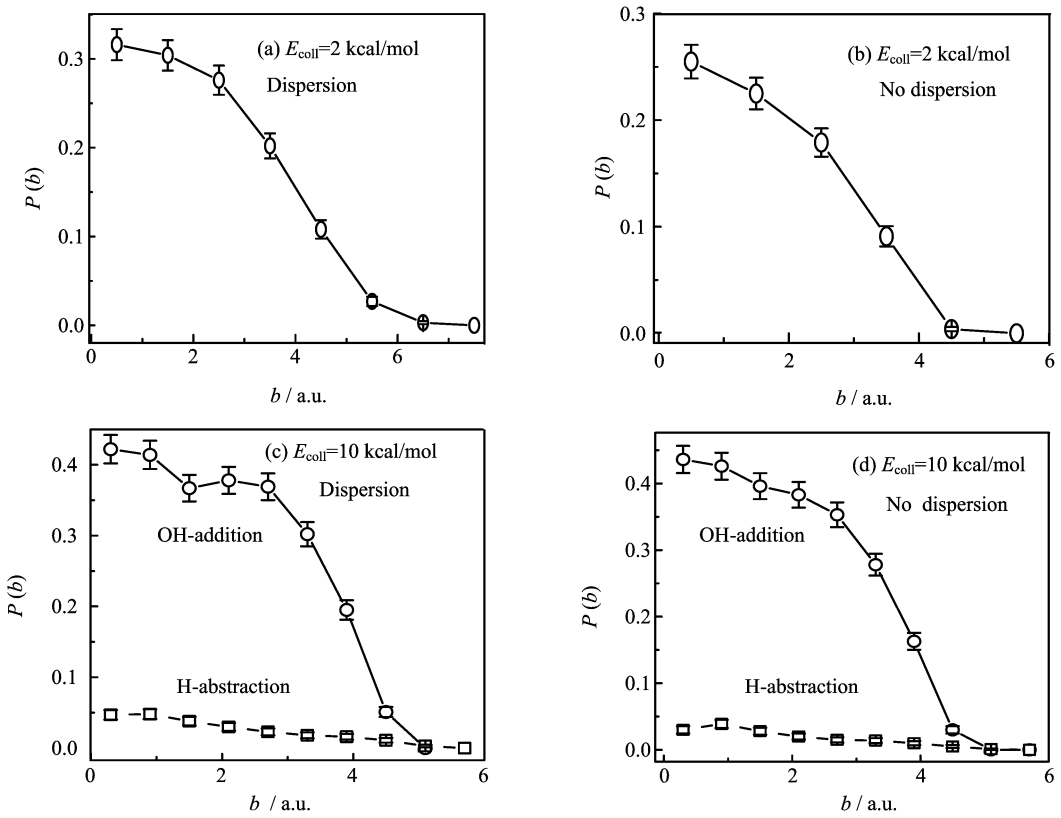

FIG. 4 Opacity functions (reaction probability $P(b)$ at impact parameter b *vs.* impact parameter) for the OH-addition and H-abstraction reaction pathways at E_{coll}=2 kcal/mol (a, b) and 10 kcal/mol (c, d). (a, b) and (c, d) are with and without dispersion correction, respectively. The reaction probabilities $P(b)$ for H-abstraction at 2 kcal/mol are insignificant and have been omitted for clarity.

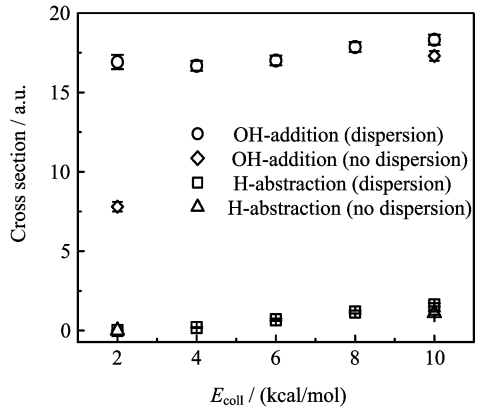

FIG. 5 Excitation functions (cross section *vs.* collision energy) for the OH-addition and H-abstraction reaction pathways of the OH+C_2H_4 reaction.

cross sections are remarkable, especially at low collision energies. With dispersion included, the cross section of OH-addition is about two times larger than that without dispersion correction at E_{coll}=2 kcal/mol. On the other hand, the cross sections with and without dispersion are comparable for addition at 10 kcal/mol. This behavior follows the differences in the opacity functions discussed above. As shown in Fig.4, at 2 kcal/mol dispersion substantially increases the maximum impact parameter for OH-addition, which results in a significantly larger cross section [48]. On the other hand, dispersion has an essentially negligible effect on either the opacity function or the maximum impact parameter at 10 kcal/mol. The cross sections for the H-abstraction channel with or without dispersion corrections at both 2 and 10 kcal/mol are statistically identical, which implies that dispersion plays no discernible role for this pathway in the OH+C_2H_4 reaction.

While there have been no experiments reported to address the excitation or opacity functions of the title reaction, thermal reaction rate constants for the addition reaction show a negative dependence on temperature [49], which is commonly interpreted as the reaction having a negative activation energy. A negative activation energy indicates a barrierless process characterized by capture-type behavior. Both the increase in reaction probability at high impact parameters and the increase of the cross sections with decreasing collision energies near the threshold in our dynamics studies point toward capture-type dynamics for the addition channel. This result is in agreement with the trend in the experimen-

DOI:10.1063/1674-0068/26/06/765-773

tal rate-constant dependence on temperature, and the potential energy profile for this pathway in Fig.3.

It should be noted that the values of the cross sections of H-abstraction pathway are generally very small and this poses an operational challenge in the direct dynamics simulations since an unusually large number of trajectories needs to be calculated to obtain state-to-state information with statistical significance. In addition, even though we generated a large number of reactive collisions forming the im1 intermediate following OH addition, none of the trajectories progressed past the im1 minimum toward products even when we increased the trajectory propagation time to several picoseconds. This is consistent with the high barriers required to exit the minimum, and suggests that regular trajectory calculations starting from reagents will be computationally very challenging if the dynamics of the progress of im1 toward products is to be studied.

V. CONCLUSION

We have investigated the reaction of the hydroxyl radical with ethene using electronic structure theory and chemical dynamics simulations evolved with a specific-reaction-parameter semiempirical Hamiltonian.

The detailed doublet potential energy surface of the OH+C_2H_4 reaction has been characterized at the MP2/aug-cc-pVDZ and CCSD(T)/aug-cc-pVTZ levels of theory. Extensive grid of high-quality *ab initio* information covering various regions of the OH+C_2H_4 PES have been used to reoptimize the original parameters of the MSINDO semiempirical Hamiltonian and obtain an SRP-MSINDO Hamiltonian suitable for the OH+C_2H_4 reaction. The empirical parameter set specific to this reaction endows the MSINDO Hamiltonian with a good degree of accuracy in comparison with the CCSD(T)/aug-cc-pVTZ energies, especially for the areas of PES around the OH-addition reaction pathway, which has a central interest in the studies reported here. An empirical damped dispersion correction was included in the development of the SRP-Hamiltonian method, and it clearly improved the description of the original MSINDO Hamiltonian in the long-range attraction region.

By using the derived SRP-MSINDO Hamiltonian, we have carried out a direct dynamics quasiclassical trajectory study of the OH+C_2H_4 reaction. The opacity functions and excitation functions stemming from the trajectory calculations show that the OH-addition channel dominates over hydrogen abstraction throughout the range of collision energies covered in this work. For OH addition, the dispersion correction plays an important role at low collision energy, whereas its contribution is less important at higher energies. This results from the increase of the relative velocity between the reagents as the collision energy increases, which overwhelms the weak attractive interaction as OH approaches the C_2H_4 molecule.

The strategy of reparameterizing a semiempirical Hamiltonian adopted in this work results in a fast and accurate electronic structure method and represents an attractive avenue to enable dynamics studies of relatively large chemical reactions. We will continue investigating the performance of this SRP-MSINDO Hamiltonian on the rest of the reaction channels on the PES of OH+C_2H_4 reaction, with the potential for predicting the dynamics of processes subsequent to the generation of the OH-addition adduct. Caution should be used in the utilization of the SRP-MSINDO Hamiltonian developed in this work for other reactions, and the general accuracy of the Hamiltonian in homologous OH+n-alkene reactions will be addressed by future trajectory simulations.

The present calculations are expected to stimulate further laboratory investigations of the atmospherically relevant hydroxyl radical reactions with alkenes, for which there are only limited reaction dynamics reports available in experimental and theoretical studies.

VI. ACKNOWLEDGMENTS

This work was supported by the National Science Foundation Grant (No.CHE-0547543), Air Force Office of Scientific Research Foundation Grant (No.FA9550-06-1-0165), and the Institute of Chemistry, Chinese Academy of Sciences (No.CMS-PY-201316).

Supplementary material: Electronic structure theory energies of stationary points for the OH+C_2H_4 reaction obtained at various levels of theory and comparison with recent theoretical results, and the opacity functions of OH-addition and H-abstraction reaction pathways at $E_{\rm coll}$=4, 6, and 8 kcal/mol.

[1] R. Atkinson and J. Arey, Chem. Rev. **103**, 4605 (2003).
[2] D. E. Heard and M. J. Pilling, Chem. Rev. **103**, 5163 (2003).
[3] J. H. Seinfeld and S. N. Pandis, *Atmospheric Chemistry and Physics: From Air Pollution to Climate Change*, New York: Wiley, (1998).
[4] K. Bolton, W. L. Hase, and G. H. Peslherbe, *Multidimensional Molecular Dynamics Methods*, D. L. Thompson, Ed., London: World Scientific Publishing, Inc., 143 (1998).
[5] D. Troya, Theor. Chem. Acc. **131**, 1072 (2012).
[6] D. Troya, M. Mosch, and K. A. O'Neill, J. Phys. Chem. A **113**, 13863 (2009).
[7] J. Zhang and W. L. Hase, J. Phys. Chem. A **114**, 9635 (2010).
[8] J. Zhang, U. Lourderaj, S. V. Addepalli, W. A. de Jong, and W. L. Hase, J. Phys. Chem. A **113**, 1976 (2009).

DOI:10.1063/1674-0068/26/06/765-773

[9] E. E. Greenwald, S. W. North, Y. Georgievskii, and S. J. Klippenstein, J. Phys. Chem. A **109**, 6031 (2005), and the references therein.
[10] J. P. Senosiain, S. J. klippenstein, and J. A. Miller, J. Phys. Chem. A **110**, 6960 (2006), and the references therein.
[11] H. Hippler and B. Viskolcz, Phys. Chem. Chem. Phys. **2**, 3591 (2000).
[12] R. S. Zhu, J. Park, and M. C. Lin, Chem. Phys. Lett. **408**, 25 (2005).
[13] G. Liu, Y. Ding, Z. Li, Q. Fu, X. Huang, C. Sun, and A. Tang, Phys. Chem. Chem. Phys. **4**, 1021 (2002).
[14] C. S. V. Aviyente, J. Mol. Model. **7**, 398 (2001).
[15] M. C. Piqueras, R. Crespo, I. Nebot-Gil, and F. Tomás, J. Mol. Struc.: THEOCHEM **537**, 199 (2001).
[16] H. B. Schlegel and C. Sosa, J. Am. Chem. Soc. **109**, 4193 (1987).
[17] H. B. Schlegel and C. Sosa, J. Am. Chem. Soc. **109**, 7007 (1987).
[18] S. E. Taylor, A. Goddard, M. A. Blitz, P. A. Cleary, and D. E. Heard, Phys. Chem. Chem. Phys. **10**, 422 (2008).
[19] J. Mikosch, S. Trippel, C. Eichhorn, R. Otto, U. Lourderaj, J. X. Zhang, W. L. Hase, M. Weidemüller, and R. Wester, Science **319**, 183 (2008).
[20] L. Sun, K. Song, and W. L. Hase, Science **296**, 875 (2002).
[21] J. G. López, G. Vayner, U. Lourderaj, S. V. Addepalli, S. Kato, W. A. deJong, T. L. Windus, and W. L. Hase, J. Am. Chem. Soc. **129**, 9976 (2007).
[22] W. L. Hase, Science **266**, 998 (1994).
[23] J. Zhang, J. Mikosch, S. Trippel, R. Otto, M. Weidemüller, R. Wester, and W. L. Hase, J. Phys. Chem. Lett. **1**, 2747 (2010).
[24] J. P. Layfield, M. D. Owens, and D. Troya, J. Chem. Phys. **128**, 194302 (2008).
[25] J. P. Layfield, A. F. Sweeney, and D. Troya, J. Phys. Chem. A **113**, 4294 (2009).
[26] W. A. Alexander, J. R. Morris, and D. Troya, J. Phys. Chem. A **113**, 4155 (2009).
[27] U. Tasić, P. Hein, and D. Troya, J. Phys. Chem. A **111**, 3618 (2007).
[28] D. Troya and E. Garcia-Molina, J. Phys. Chem. A **109**, 3015 (2005).
[29] D. Troya and P. J. E. Weiss, J. Chem. Phys. **124**, 074313 (2006).
[30] D. Troya, J. Phys. Chem. A **109**, 5814 (2005).
[31] D. Troya, J. Chem. Phys. **123**, 214305 (2006).
[32] T. Bredow and K. Jug, Theor. Chem. Acc. **113**, 1 (2005).
[33] A. Gonzalez-lafont, T. N. Truong, and D. G. Truhlar, J. Phys. Chem. **95**, 4618 (1991).
[34] W. J. Hehre, L. Radom, P. V. R. Schleyer, and J. A. Pople, *Ab initio Molecular Orbital Theory*, New York: Wiley (1986).
[35] G. F. Adams, G. D. Bent, R. J. Bartlett, and G. D. Purvis, *Potential Energy Surfaces and Dynamics Calculations*, D. G. Truhlar, Ed., New York: Plenum, 133, (1981).
[36] T. H. Jr. Dunning, J. Chem. Phys. **90**, 1007 (1989).
[37] D. E. Woon and T. H. Jr. Dunning, J. Chem. Phys. **98**, 1358 (1993).
[38] K. Fukui, Acc. Chem. Res. **14**, 363 (1981).
[39] K. Raghavachari, G. W. Trucks, J. A. Pople, and M. Head-Gordon, Chem. Phys. Lett. **157**, 479 (1989).
[40] M. J. Frisch, G. W. Trucks, H. B. Schlegel, G. E. Scuseria, M. A. Robb, J. R. Cheeseman, G. Scalmani, V. Barone, B. Mennucci, G. A. Petersson, H. Nakatsuji, M. Caricato, X. Li, H. P. Hratchian, A. F. Izmaylov, J. Bloino, G. Zheng, J. L. Sonnenberg, M. Hada, M. Ehara, K. Toyota, R. Fukuda, J. Hasegawa, M. Ishida, T. Nakajima, Y. Honda, O. Kitao, H. Nakai, T. Vreven, J. A. Jr. Montgomery, J. E. Peralta, F. Ogliaro, M. Bearpark, J. J. Heyd, E. Brothers, K. N. Kudin, V. N. Staroverov, R. Kobayashi, J. Normand, K. Raghavachari, A. Rendell, J. C. Burant, S. S. Iyengar, J. Tomasi, M. Cossi, N. Rega, J. M. Millam, M. Klene, J. E. Knox, J. B. Cross, V. Bakken, C. Adamo, J. Jaramillo, R. Gomperts, R. E. Stratmann, O. Yazyev, A. J. Austin, R. Cammi, C. Pomelli, J. W. Ochterski, R. L. Martin, K. Morokuma, V. G. Zakrzewski, G. A. Voth, P. Salvador, J. J. Dannenberg, S. Dapprich, A. D. Daniels, Ö. Farkas, J. B. Foresman, J. V. Ortiz, J. Cioslowski, and D. J. Fox, *Gaussian 09*, Inc., Wallingford CT: Gaussian, Inc., (2009).
[41] B. Ahlswede and K. Jug, J. Comput. Chem. **20**, 563 (1999).
[42] B. Ahlswede and K. Jug, J. Comput. Chem. **20**, 572 (1999).
[43] D. Skouteris, D. E. Manolopoulos, W. S. Bian, H. J. Werner, L. H. Lai, and K. P. Liu, Science **286**, 1713 (1999).
[44] S. Grimme, J. Comput. Chem. **25**, 1463 (2004).
[45] S. Grimme, J. Comput. Chem. **27**, 1787 (2006).
[46] W. L. Hase, R. J. Duchovic, X. Hu, A. Komornicki, K. F. Lim, D. H. Lu, G. H. Peslherbe, K. N. Swamy, S. R. Vande Linde, A. Varandas, H. Wang, and R. J. Wolf, Quantum Chem. Program Exchange Bull. **16**, 671 (1996).
[47] X. Hu, W. L. Hase, and T. Pirraglia, J. Comput. Chem. **12**, 1014 (1991).
[48] R. D. Levine, *Molecular Reaction Dynamics*, Cambridge, UK, New York: Cambridge University Press (2005).
[49] E. W. G. Diau and Y. P. Lee, J. Chem. Phys. **96**, 377 (1992).
[50] D. R. Lide, *CRC Handbook of Chemistry and Physics*, 83th Edn., London: DRC Press LLC, 9 (2002).
[51] T. Shimanouchi, "Molecular Vibrational Frequencies" in NIST Chemistry WebBook, NIST Standard Reference Database Number 69, P. J. Linstrom and W. G. Mallard, Eds., National Institute of Standards and Technology, 20899. (http://webbook.nist.gov)

DOI:10.1063/1674-0068/26/06/765-773